Coulomb Excitation of ^{209}Bi and the Weak-Coupling Model*

R. A. Broglia, J. S. Lilley, R. Perazzo, and W. R. Phillips†

School of Physics and Astronomy, University of Minnesota, Minneapolis, Minnesota 55455

(Received 19 June 1969)

Some relative and absolute γ-ray transition probabilities have been measured for the low-lying levels in ^{209}Bi by observing the Coulomb excitation and subsequent decay of the states. Thick bismuth targets were bombarded with 19-MeV α particles, and γ-ray yields at 0°, 30°, 45°, 60°, and 90° were observed with a 25-cm³ LiGe detector. Determinations have been made of the transition strengths to the $f_{7/2}$ (0.897-MeV), the $i_{13/2}$ (1.608-MeV), the $f_{5/2}$ (2.822-MeV), and the septuplet of levels near 2.6 MeV, formed by coupling an $h_{9/2}$ particle to the 3⁻ octupole state in ^{208}Pb, excited by $E2$, $E3$, $E2$, and $E3$ Coulomb excitation, respectively. Approximate $E1$ transition strengths for ground-state decays of the 2.563-, 2.581-, and 2.598-MeV levels have been determined from the Doppler broadening of the γ peaks. Branches are observed corresponding to decays from the 2.741- and 2.600-MeV states to the 1.608 ($\frac{13}{2}^+$) level, and from the 2.822-, 2.615-, and 2.581-MeV levels to the 0.897 ($\frac{7}{2}^-$) state. The γ-ray strengths and relative transition rates are compared with the predictions of a particle-vibration coupling model.

I. INTRODUCTION

IN recent years, a considerable amount of attention has been directed towards obtaining a detailed understanding of nuclei near the doubly magic nucleus ^{208}Pb. Here one finds quite pure shell-model configurations for the low-lying states of the neighboring nuclei.[1-4] In addition, multiplets of levels formed by coupling the single-particle configurations to the collective states of the ^{208}Pb core are observed[5,6] and are well described by the weak-coupling model.[7]

In this paper, we are concerned with the states of ^{209}Bi. The ground state, with spin and parity $\frac{9}{2}^-$, is well described as an $h_{9/2}$ single proton coupled to the ground state of ^{208}Pb. Multiplets formed by coupling this proton to the 3⁻ and 5⁻ core states have been observed, grouped close to the excitation energies of the core states.[6] The summed transition strengths to the members of the multiplets are roughly equal to the strengths for corresponding transitions to the core states. This fact and the fact that the multiplets show little splitting suggest that the particle-vibration coupling is very weak.[8] The three other states in ^{209}Bi below 3 MeV are strongly populated in single-proton

transfer reactions on ^{208}Pb.[2-4] These are the $f_{7/2}$ (0.89 MeV), the $i_{13/2}$ (1.61 MeV) and the $f_{5/2}$ (2.83 MeV) single-proton states expected from the shell model. The $p_{3/2}$ and $p_{1/2}$ states also expected in the $Z=82-126$ shell have been identified and lie at 3.1 and 3.6 MeV, respectively.

At present, there is little detailed information on the coupling of particles to vibrations in this region. The splitting of the multiplets is due to this coupling, and the (3⁻, $h_{9/2}$) multiplet in ^{209}Bi near 2.6 MeV has been discussed by several authors.[8,9] All but two of the states have been resolved in recently reported experiments on inelastic scattering.[6]

Particle-vibration coupling also may be studied by detecting small admixtures of single-particle states in states of the multiplet and vice versa. Evidence of the former mixing has been noted in the single-proton transfer reactions to the octupole multiplet in the ^{208}Pb$(\alpha, t)^{209}$Bi reaction[3] and in recent (^{3}He, d) experiments.[4] It is most probable that the transitions are to the $i_{11/2}$ and $i_{13/2}$ multiplet members, indicating admixtures of the $i_{11/2}$ and $i_{13/2}$ single-particle states into the multiplet states. That the $i_{13/2}$ state at 1.61 MeV has collective state admixtures is supported by the studies of inelastic scattering where the strength of the inelastic group to the $i_{13/2}$ state is observed to be enhanced about 30 times over that expected for a single-particle state.[8]

In order to pursue the study of these and other effects in more detail, we present the results of an experiment in which γ-transition strengths and branching ratios are determined following the Coulomb excitation of ^{209}Bi with 19-MeV α particles. The results are compared in detail with calculations using wave functions based on the weak-coupling model. γ-transition rates are sensitive to small admixtures in the wave functions and so provide a critical test of the theory.

Previous Coulomb-excitation experiments on ^{209}Bi[10-12]

† Present address: Dept. of Physics, University of Manchester, Manchester, England.

[1] P. Mukherjee and B. L. Cohen, Phys. Rev. **127**, 1284 (1962); W. R. Hering and M. Dost, Phys. Letters **19**, 488 (1965); S. Hinds, R. Middleton, J. H. Bjerregaard, O. Hansen, and O. Nathan, Nucl. Phys. **83**, 17 (1966); G. Muehllehner, A. S. Poltorak, W. C. Parkinson, and R. H. Bassel, Phys. Rev. **159**, 1039. (1967).

[2] R. Woods, P. D. Barnes, E. R. Flynn, and G. J. Igo, Phys. Rev. Letters **19**, 453 (1967); B. H. Wildenthal, B. M. Preedom, E. Newman, and M. R. Cates, *ibid.* **19**, 960 (1967).

[3] J. S. Lilley and Nelson Stein, Phys. Rev. Letters, **19**, 709 (1967).

[4] C. Ellegaard and P. Vedelsby, Phys. Letters **26B**, 155 (1968); J. Bardwick and R. Tickle, Phys. Rev. **171**, 1305 (1968).

[5] J. Alster, Phys. Rev. **141**, 1138 (1966); S. Hinds, H. Marchant, J. H. Bjerregaard, and O. Nathan, Phys. Letters **20**, 674 (1966).

[6] J. C. Hafele and R. Woods, Phys. Letters **23**, 579 (1966).

[7] A. De Shalit, Phys. Rev. **122**, 1530 (1961).

[8] B. R. Mottelson, J. Phys. Soc. Japan Suppl. **24**, 87 (1968).

[9] J. C. Hafele, Phys. Rev. **159**, 996 (1967).

[10] O. Nathan, Nucl. Phys. **30**, 332 (1962).

[11] S. Berko, Bull. Am. Phys. Soc. **4**, 414 (1959).

[12] A. Z. Hrynkiewicz, S. Szymczyk, T. Walczak, G. Zapalski, F. Baldeweg, and G. Stiller, Phys. Letters **6**, 326 (1963).
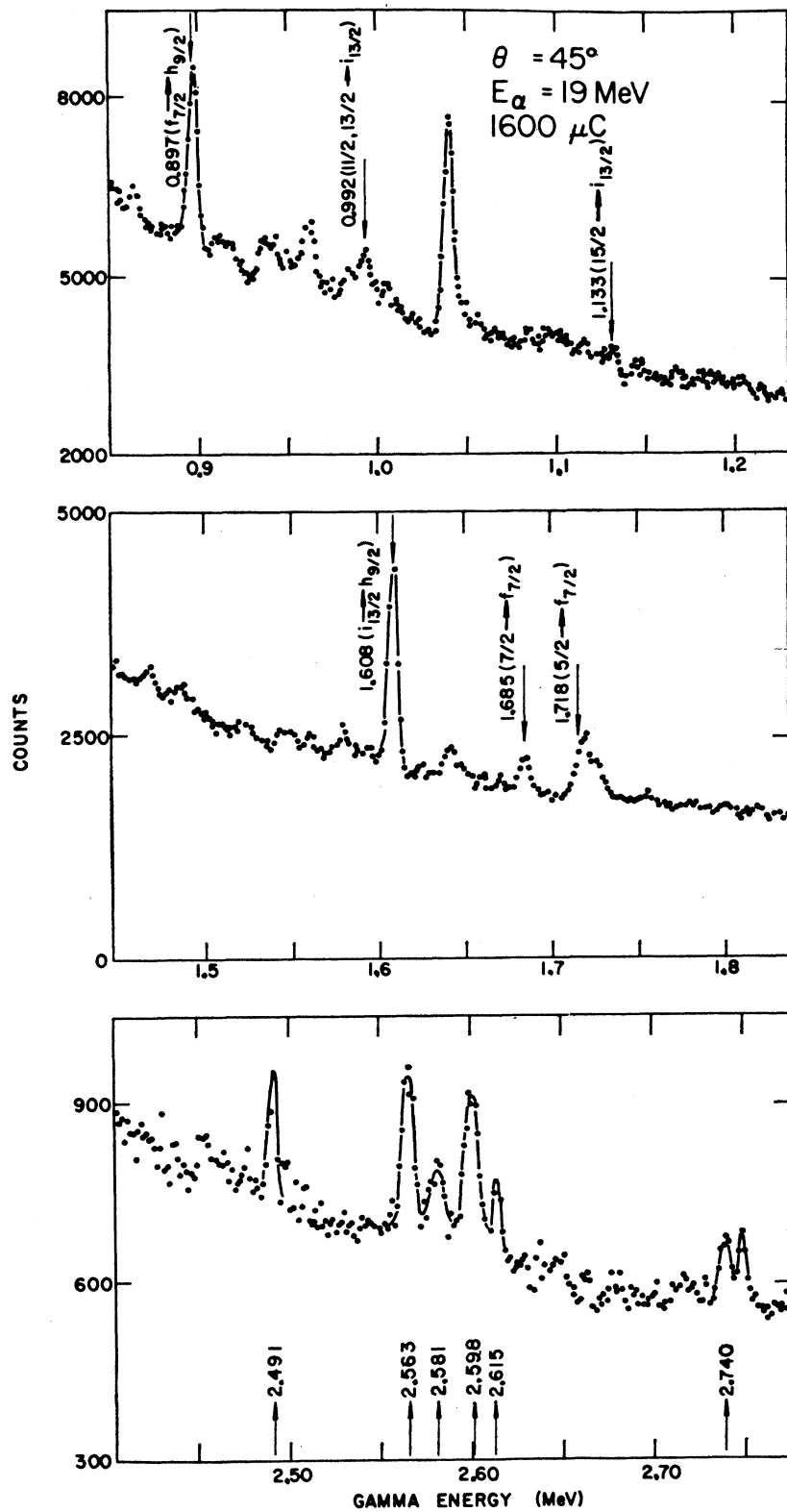
FIG. 1. Energy spectra of γ rays emitted at 45° from bismuth bombarded with 19-MeV α particles.
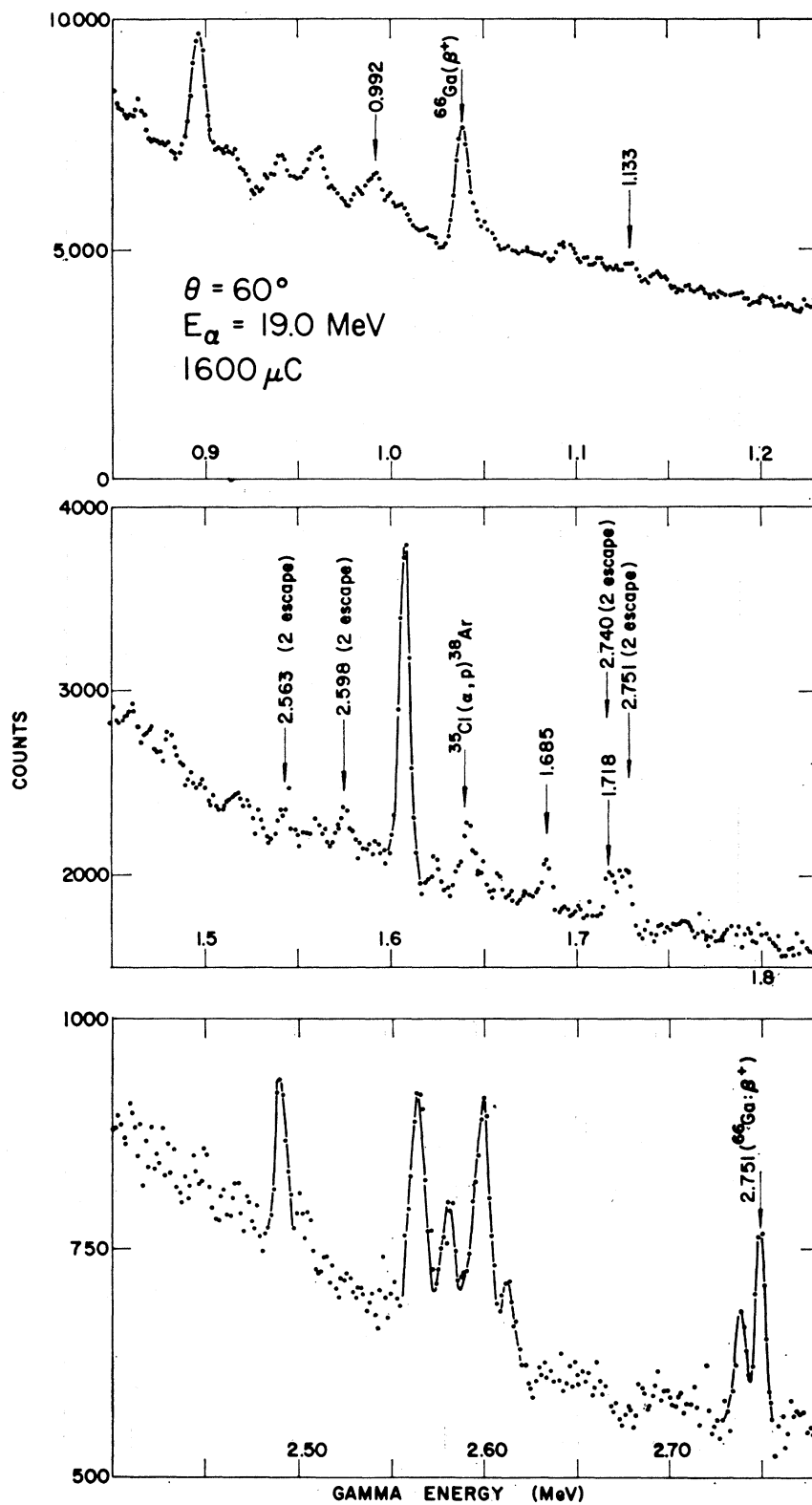
FIG. 2. Energy spectra of γ rays emitted at 60° from bismuth bombarded with 19-MeV α particles.
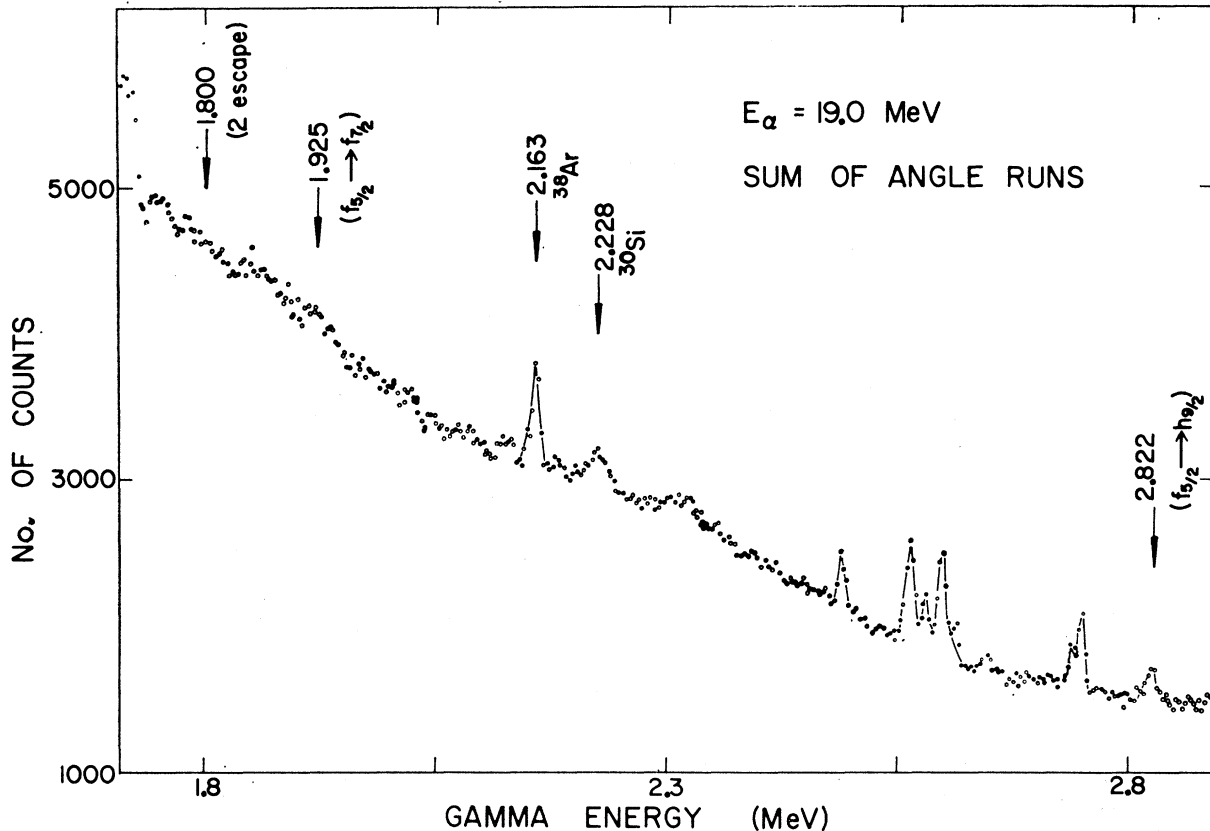
FIG. 3. Summed energy spectrum of γ rays emitted from bismuth bombarded with 19-MeV α particles. The spectrum is a weighted sum of data taken at 0°, 30°, 45°, 60°, and 90°.

have been severely handicapped by the poor energy resolution of NaI γ-rays detectors. In only one of these experiments[12] was an attempt made to observe γ rays from states higher than the 0.89-MeV level. That experiment reported an enhancement of the E3 transition from the ground state to the 1.61-MeV state; however, their measurement is only approximate due to inability to take into account the cascade feeding of the 1.61-MeV level from states above it. During the course of the present experiment, preliminary results on the Coulomb excitation of ^{209}Bi with oxygen ions were reported.[13] There are some advantages to exciting the levels with ^{4}He particles: The recoil Bi nuclei have less velocity, and thus the Doppler broadening of γ rays from short-lived levels is smaller, so that γ-ray lines overlap less. Also, possible second-order contributions to the Coulomb-excitation amplitude are less serious with ^{4}He than with heavier projectiles.

II. EXPERIMENTAL

Thick targets of chemically pure bismuth were bombarded with ^{4}He particles to produce a source of excited ^{209}Bi levels. The γ decays of these states were

observed with a lithium-drifted germanium detector whose nominal active volume was about 25 cm^3. The targets were foils, rolled to a thickness of 0.010 in., whose surfaces were scraped clean before insertion in the target chamber in order to minimize oxygen and carbon surface contaminants. The chief backgrounds during the experiment still came from oxygen and carbon. Other slight contaminants in the target which gave identifiable background γ rays from (α, p) or (α, n) reactions (and from ensuing activities in some cases) were Si, Cl, and Cu. The strongest background lines are identified in one or other of the γ spectra shown in Figs. 1–3. These γ rays were identified from their energies and from their association with other background lines.[14,15]

The experimental measurements consisted of two sets. One was a set of spectra taken for $E_\alpha = 19.0$ MeV and mean angles of observation θ of 0°, 30°, 45°, 60°, and 90° to the beam direction. The solid angle subtended at the target by the *front face* of the detector during these runs was approximately 0.35 sr, and for

[13] J. P. Schiffer, D. G. Fleming, H. E. Gove, and J. Hertel, Bull. Am. Phys. Soc. **13**, 655 (1968).

[14] C. M. Lederer, J. M. Hollander, and I. Perlman, in *Table of Isotopes* (John Wiley & Sons, Inc., New York, 1967).

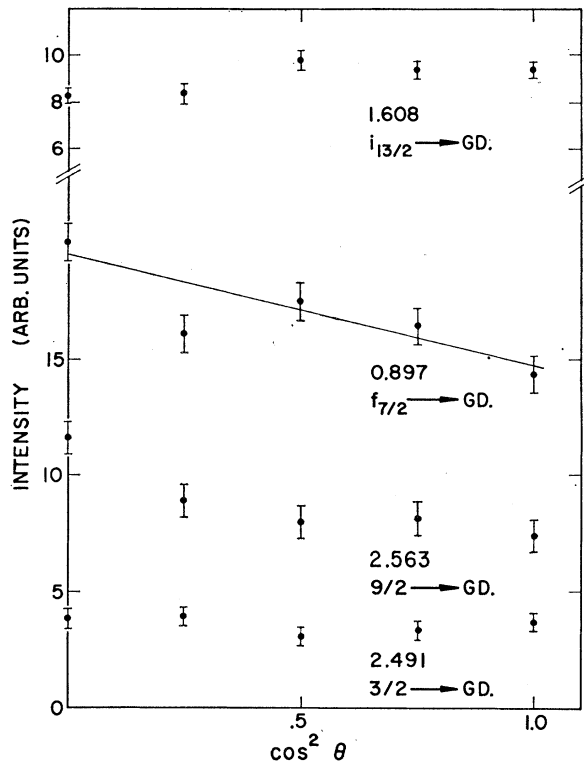[15] P. M. Endt and C. van Der Leun, Nucl. Phys. **A105**, 1 (1967).

FIG. 4. Angular distributions of the 1.608-, 0.897-, 2.563-, and 2.491-MeV γ rays from bismuth at 19 MeV. The solid line was calculated assuming that the 0.897-MeV ($\frac{7}{2}^-$) state is formed via $E2$ Coulomb excitation and decays via an $E2/M1$ mixture. The $E2/M1$ intensity ratio was taken to be unity, and the de-excitation γ rays due to population from higher levels were assumed to be isotropic.

each run the target was bombarded with 1.6 mCi of He^{++}. The other set of measurements was taken with the counter at 45°, and the thick-target yields of the γ rays were measured for $E_\alpha = 18.5$, 19.0, and 19.5 MeV.

The identification of the γ lines from the decays of the ^{209}Bi levels was made on the basis of their energies and because their yields as a function of the ^{4}He energy varied in the manner expected from the Coulomb-excitation process (see Sec. III A). The energies of the sharper γ-ray lines were measured to ±0.5 keV when all the data sets were used.

Figures 1 and 2 show portions of the γ-ray spectra observed at 45° and 60° with $E_\alpha = 19.0$ MeV. γ rays from the ^{209}Bi excitations and some background lines are labeled. Figure 3 shows a spectrum which is compressed to cover the γ-ray energy range 1.6–3.0 MeV; it is the sum of all the angle runs taken at 19.0 MeV and illustrates the presence of γ rays from the "$f_{5/2}$" level at 2.82 MeV. The lifetime of this state is much shorter than those of most of the other ^{209}Bi levels excited, and so the summed γ-ray peak is correspondingly broadened.

Angular distributions shown in Figs. 4–6 are featureless and contain no terms higher than $P_2(\cos\theta)$ to the accuracy with which we have measured them. The total intensity of a particular γ ray was obtained from

these curves (knowing the total peak efficiency of the detector). The efficiency was obtained by calibrating the detector with sources of ^{56}Co and ^{60}Co, which were standardized by using a NaI crystal whose efficiency was calculable.[16] The detector efficiency for 2.6-MeV γ rays was 1.8×10^{-4}, to within an accuracy of ±10%.

Figure 7 shows the energy-level scheme of ^{209}Bi and the γ decays observed in this experiment. The energies of the levels are those measured in this experiment and are accurate to ±0.5 keV, except for the 2.598-, 2.581-, and 2.563-MeV levels, which are believed accurate to ±1.0 keV. The numbers quoted in Fig. 7 for the total intensities are the numbers in units of 10^6 of the various γ rays emitted from a thick target of Bi when bombarded with 1.6 mCi of 19.0-MeV ^{4}He^{++}.

III. ANALYSIS

A. Excitation Mechanism

The values of the reduced matrix elements for the upward $E3$ and $E2$ transitions can be calculated from the measured thick-target yields by using Coulomb-excitation theory,[17] provided that one is sure that it is
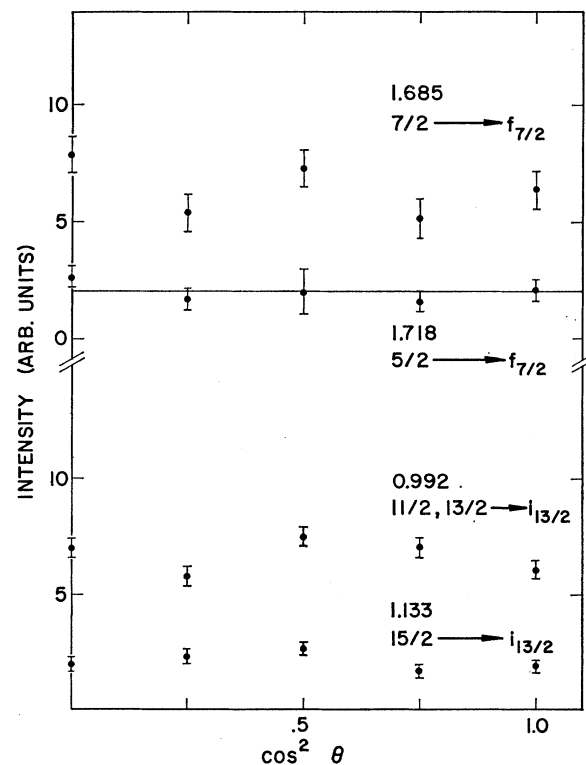
FIG. 5. Angular distributions of 1.685-, 1.718-, 0.992-, and 1.133-MeV γ rays from bismuth at 19 MeV. The solid line was calculated assuming pure electric-dipole decay to the $\frac{7}{2}^-$ state following $E3$ Coulomb excitation of the $\frac{9}{2}^+$ state.

[16] *Alpha-, Beta-, and Gamma-Ray Spectroscopy*, edited by K. Siegbahn (North-Holland Publishing Co., Amsterdam, 1965).

[17] K. Alder, A. Bohr, J. Huus, B. Mottleson, and A. Winther, Rev. Mod. Phys. **28**, 432 (1956).

only the Coulomb field responsible for those upward transitions. It is known that, for 19-MeV ⁴He on ²⁰⁸Pb, the excitation of the 3⁻ state at 2.6 MeV shows appreciable deviation from simple Coulomb excitation. This is probably due to a direct nuclear process. However, at 18 MeV the observations are consistent with Coulomb excitation alone.[18] For a thick Bi target and E3 excitation of levels around 2.6 MeV, more than one-half of the thick-target yield comes from α particles with energies less than 18 MeV. Thus it may be expected that our data can be interpreted in terms of Coulomb excitation alone, and in this section we present evidence that this is so.

Figure 8 shows parts of the γ spectra taken at different ⁴He bombarding energies. From these spectra, the thick-target yields of the 1.608- and 0.897-MeV γ rays were extracted.[19] The thick-target yields are
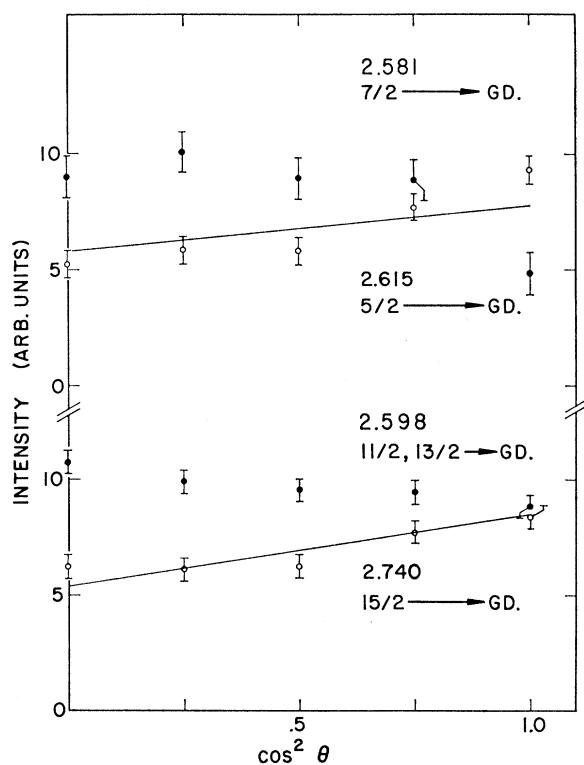

FIG. 6. Angular distributions of 2.581-, 2.615-, 2.598-, and 2.740-MeV γ rays from bismuth at 19 MeV. The solid-line fit to the 2.740-MeV distribution was made assuming pure E3 decay following E3 Coulomb excitation of the 15/2⁺ state. The fit to the 2.615-MeV distribution was given by E3 excitation of the $\frac{5}{2}^+$ state with an E3/M2 intensity ratio of 4 in the ground-state decay.

---

[18] A. R. Barnett and W. R. Phillips, Phys. Rev. **186**, 1205 (1969).

[19] The thick-target yields involve integrating over all solid angle. In order to obtain thick-target yields from measurements at 45°, corrections were made based on the angular distributions observed at a bombarding energy of 19.0 MeV. The angular distributions are slowly varying functions of the incident energy, as calculation of the angular-distribution coefficients shows, and so little error should be introduced by this procedure.
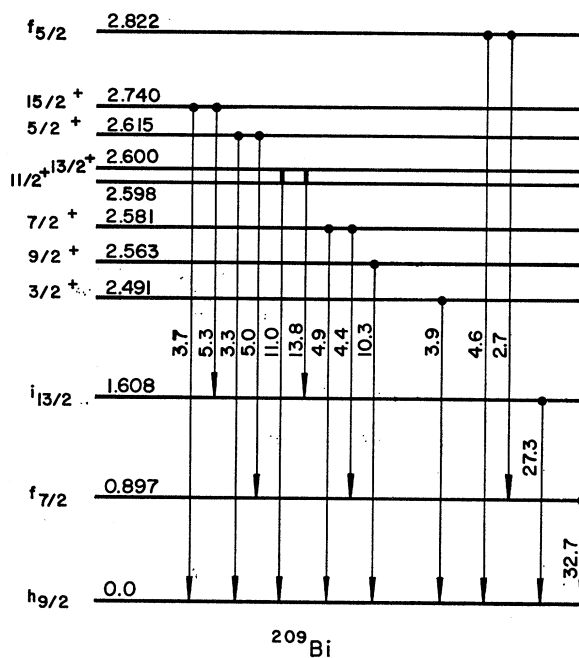

FIG. 7. Energy-level scheme of ²⁰⁹Bi showing the observed γ transitions and numbers in units of 10⁶ of the various γ rays emitted from a thick target of bismuth when bombarded with 1.6 mCi of He.⁺⁺ The energies quoted are those determined in this experiment.

shown in Fig. 9 as a function of incident ⁴He energy. The full lines on the figure are the theoretical predictions for the thick-target yields of the two γ rays and are based on the assumption of Coulomb excitation alone for the excitation mechanism. They involve the branching ratios of higher levels to the 1.608- and 0.897-MeV states. These were determined from the data given on Fig. 7. They also involve the strengths of the upward transitions, which were determined from the set of data at 19.0 MeV, with this set analyzed *as if the excitation were Coulomb excitation alone*. Thus, Fig. 9 supports the view that electric excitation is the only process we need consider, and, further, is a consistency check on the treatment and analysis of the data sets.

The identification of other less intense Bi γ-ray lines was corroborated by the observation of their expected yields as a function of α-particle energy, as mentioned in Sec. II.

The Coulomb-excitation theory used in the analysis of the experimental data is the symmetrized semi-classical theory reviewed by Alder *et al.*[17] No "exact" quantum-mechanical calculations exist for E3 excitation, but the semiclassical theory should be valid, as the value of the Sommerfeld parameter η was about 12 in these experiments. The symmetrization of the classical expressions, however, leaves a little uncertainty, and has never been tested to any great accuracy, especially for E3 excitations (very few examples of
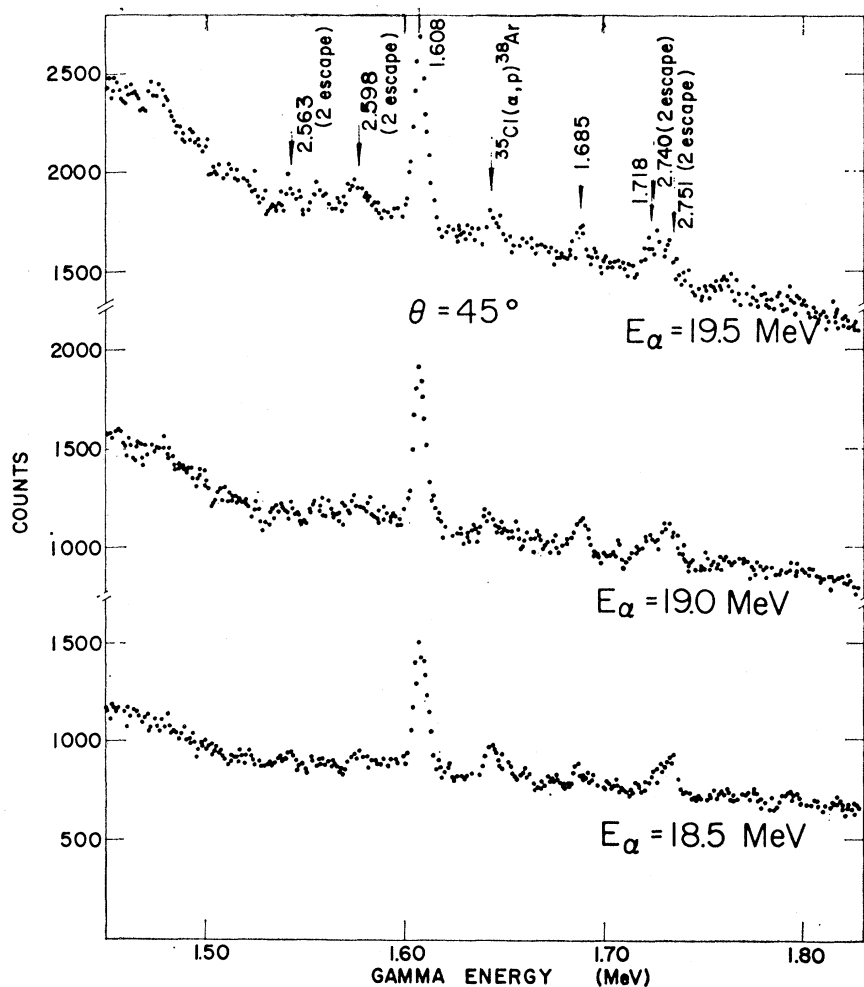
FIG. 8. Energy spectra of γ rays near 1.6 MeV emitted at 45° from bismuth bombarded with 18.5-, 19.0-, and 19.5-MeV α particles.

which exist in the literature).[20,12] A different symmetrization procedure could alter significantly the predicted cross sections and so give different reduced matrix elements when our data are compared. The only other symmetrization procedure suggested produces no different predictions.[21] An important result in this experiment is the comparison of the summed $E3$ strength to the octupole multiplet compared to the $E3$ strength from ground to 3⁻ in ^{208}Pb. Both of these values will have been obtained using the same Coulomb-excitation theory.

One other effect which should be considered is the possibility that second-order terms in the perturbation expression for the cross sections may influence the predicted total cross sections or angular distributions. These effects can be large for $E3$ excitations, especially

with heavy ions. For ^{4}He, however, they are expected to be small, as in the ^{208}Pb case,[18] and we neglect them here.

B. γ-Ray Lifetimes

The γ peaks due to the ground-state transitions from the 2.563-, 2.581-, 2.598-, and 2.822-MeV states are broadened and shifted by the Doppler effect. Lifetimes of the order of the slowing-down time of the emitting ions can be determined by measurements of the Doppler effect, and, if the multipolarity of a certain γ decay is known and if the fraction of a state of known lifetime that decays with emission of that γ ray is known, the reduced matrix element for the γ decay can be determined. In this experiment, lifetimes were determined by an adaptation of the Doppler-shift technique.[22,23]

Theories of the passage of heavy ions through matter give expressions for the variation of the average ion speed with time $\langle v(t) \rangle$, assuming the initial average

[20] G. A. Jones and W. R. Phillips, Proc. Roy. Soc. (London) **A239**, 487 (1957); A. E. Litherland, M. A. Clark, and C. Broude, Phys. Letters **3**, 204 (1963); A. Z. Hrynkiewicz, S. Kopta, S. Szymczyk, T. Walczak, and I. Kuzniecov, Nucl. Phys. **79**, 495 (1966); E. Veje, B. Elbek, B. Herskind, and M. C. Olesen, *ibid.* **A109**, 489 (1968).

[21] L. C. Biedenharn and P. J. Brussard, in *Coulomb Excitation* (Clarendon Press, Oxford, 1965).

[22] S. Devons, in *Nuclear Spectroscopy*, edited by F. Ajzenberg-Selove (Academic Press Inc., New York, 1960), part A.

[23] A. E. Litherland, M. J. L. Yates, B. M. Hinds, and D. Eccleshall, Nucl. Phys. **44**, 220 (1963).

speed $\langle v(0) \rangle$ is known, as it is in this case. The mean speed of the ions at the instant they emit the γ ray is

$$\langle v \rangle = \tau^{-1} \int_0^\infty \langle v(t) \rangle e^{-t/\tau} dt. \quad (1)$$

The problem is to determine $\langle v \rangle$ from the experimental data, and thence τ.

Since there are no experimental data for the slowing down of bismuth ions in bismuth, $\langle v(t) \rangle$ was calculated using theoretical formulas that were the result of work by Lindhard, Scharff, and Schiott.[24] According to these authors, the stopping power is close to a maximum over most of the range of bismuth-ion velocities considered here, and, for each level under consideration, was taken to be a constant equal to the value corresponding to the effective mean speed of the emitting ions $\langle v \rangle$. The error in this procedure was estimated to be considerably less than the accuracy quoted for the calculations themselves.[24]

Combining measurements of the Doppler shift and the Doppler broadening gave a value for the mean square velocity of the emitting ions $\langle v^2 \rangle$. In order to

TABLE I. Level energies, widths, and lifetimes from γ-ray lines.

E (keV)	Mean γ-peak width	γ-peak shift (keV)	Lifetime (10^{-13} sec)
2491±0.5	7.1±0.8	···	a
2563±1.0	10.1±0.8	4.5±1.5	0.40±0.40
2581±1.0	8.7±0.8	1.5±1.2	$2.2_{-1.0}^{+2.0}$
2598±1.0	10.6±0.7	3.5±1.2	0.45±0.40[b]
2615±0.5	7.7±0.7	···	a
2740±0.5	7.1±0.3	···	a
2751±0.5[e]	6.7±0.4	···	···
2822±2.0	11.0±2.5	6.0±2.0	<0.5[d]

[a] $\tau > 5 \times 10^{-13}$ sec.
[b] Assumes most of the ground-state γ ray comes from 11/2⁺.
[e] ⁶⁶Ga activity line sharp.
[d] Partial E2 lifetime to ground $<14^{-14}$ sec from BE2.

determine $\langle v \rangle$ from $\langle v^2 \rangle$, it was necessary to assume a form for the average distribution of ion speeds. This gives the constant k in the expression $\langle v \rangle = k \langle v^2 \rangle^{1/2}$; then, knowing $\langle v \rangle$, τ was determined from Eq. (1). k was taken to lie halfway between the values given by the initial speed distribution (0.92) and an exponential distribution (0.7). The error on k was taken to be one quarter of that range. In principle, information about the mean-velocity distribution can be obtained from the shape of the Doppler-broadened peaks at different angles. In the present case, the effects were much too small for this to be possible.

Table I shows the properties of the ground-state γ peaks from different levels. The intrinsic resolution of the detector was given by averaging the widths of the peaks due to the four other members of the multiplet that are not expected to be broadened, and the long-lived background γ at 2.751 MeV. The Doppler shifts were determined from plots of peak position as a function of angle. These are shown in Fig. 10. Only the broadened peaks show any measurable shift with angle. The lifetimes determined using the procedure described above are also shown in Table I. They complement the results of Metzger[25] for the E1 lifetimes of the 7/2⁺, 9/2⁺, and 11/2⁺ multiplet states using a resonance-fluorescence method. This technique gave the best results for the short-lived 9/2⁺ and 11/2⁺ levels where the Doppler-shift method gave only upper limits.

The major sources of error are the following: (1) The extraction of spreading widths and shifts from the data are subject to statistics and uncertainties in subtracting the background. An analysis of all the data suggests that, in general, a given measurement of the position of a peak is accurate to ±1 keV (see Fig. 10). Errors in the peak widths were estimated from the spread in values obtained at different angles, there being no evidence that the broadening is different at different angles. (2) Calculations of the slowing-down process were estimated by Lindhard et al.[24] to be accurate to
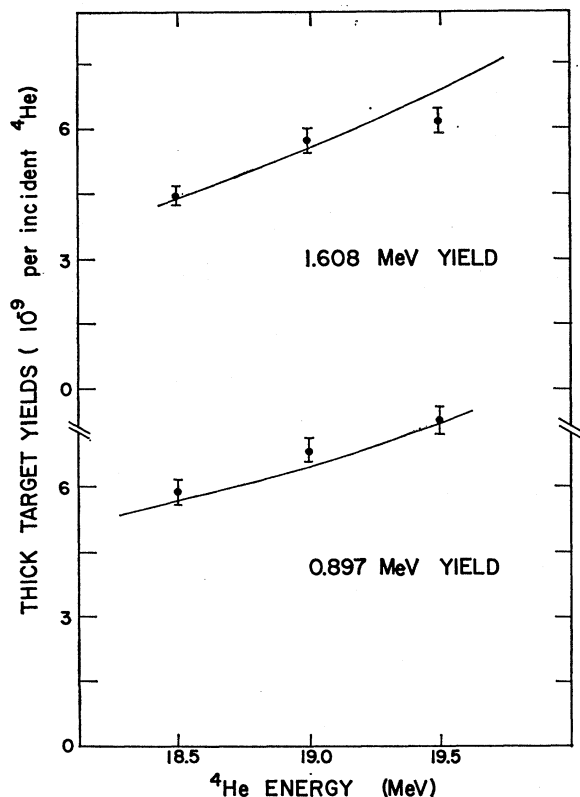

FIG. 9. Thick-target yields of the 1.608- and 0.897-MeV γ rays from bismuth as a function of α-particle bombarding energy. The solid curves are predictions based on first-order Coulomb-excitation theory using transition strengths given by an analysis of the data taken at 19.0 MeV.

[24] J. Lindhard, M. Scharff, and H. E. Schiott, Kgl. Danske Videnskab. Selskab, Mat.-Fys. Medd. **33**, No. 14 (1963).

[25] F. R. Metzger, Bull. Am. Phys. Soc. **14**, 608 (1969).

TABLE II. Reduced transition probabilities.

Transition	Type	Method of measurement	$B(EL)_{expt}$[a]	$B(EL)$ theory I[b]	$B(EL)$ theory II[c]	$\dfrac{B(EL)_{expt}}{B(EL)_{s.p.}}$ [d]
$0 \to 2.6$[e]	$E3$	γ-ray intensities	$(0.57\pm0.03)\ e^2b^3$	$\cdots$	$\cdots$	31.5
$0 \to 1.608$	$E3$	γ-ray intensities	$(1.24\pm0.32)\times10^{-2}\ e^2b^3$	$1.2\times10^{-2}\ e^2b^3$	$1.2\times10^{-2}\ e^2b^3$	0.68
$0 \to 0.897$	$E2$	γ-ray intensities	$(1.39_{-0.23}{}^{+0.16})\times10^{-3}\ e^2b^2$	$0.15\times10^{-3}\ e^2b^2$	$1.23\times10^{-3}\ e^2b^2$	3.8×10^{-2}
$0 \to 2.822$	$E2$	γ-ray intensities	$(2.90\pm1.00)\times10^{-2}\ e^2b^2$	$0.3\times10^{-2}\ e^2b^2$	$3.4\times10^{-2}\ e^2b^2$	0.79
$2.581 \to 0$	$E1$	Lifetime and γ-ray intensities[f]	$(0.90_{-0.41}{}^{+0.62})\times10^{-6}\ e^2b$	$1.25\times10^{-3}\ e^2b$	$0.9\times10^{-6}\ e^2b$ $[k(\tau=1)=4.2]$	1.3×10^{-5}
$2.581 \to 0.897$	$E1$	Lifetime and γ-ray intensities[f]	$(2.8_{-1.3}{}^{+2.0})\times10^{-6}\ e^2b$	$2\times10^{-4}\ e^2b$	$2.8\times10^{-6}\ e^2b$ $[k(\tau=1)=5.3]$	4.1×10^{-5}
$2.563 \to 0$	$E1$	Lifetime and γ-ray intensities	$\gtrsim4.5\times10^{-6}\ e^2b$	$9\times10^{-4}\ e^2b$	$8.8\times10^{-6}\ e^2b$ $[k(\tau=1)=5.5]$	$\gtrsim7\times10^{-5}$
$2.598 \to 0$	$E1$	Lifetime and γ-ray intensities	$\gtrsim4.5\times10^{-6}\ e^2b$	$2.4\times10^{-3}\ e^2b$	$1.6\times10^{-5}\ e^2b$ $[k(\tau=1)=5.5]$	$\gtrsim7\times10^{-5}$

[a] Errors quoted do not include a 10% uncertainty in absolute efficiency of detector.
[b] Calculations include coupling to the 3^- vibrational state only.
[c] Calculations include coupling to the 3^-, 2^+, and 1^- vibrational states. For the $E1$ transitions, the strength parameter $k(\tau=1)$ was adjusted to give agreement with experiment (see text).
[d] $B(E1)_{s.p.} = (2L+1)\ (e^2/4\pi)\ [3/(3+L)]^2 R_0{}^{2L}$: $R_0=1/2A^{1/3}\times10^{-13}$cm.
[e] Summed $E3$ strength to septuplet.
[f] Assumes that the $\frac{7}{2}^+$ level has significant decays to ground and $f_{7/2}$ only.

about 20%. Good agreement with experiment has been demonstrated in several instances,[26] and it is not expected that the inaccuracy in the present case will be much worse than this. (3) The error due to the assumption made for the distribution of speeds cannot be determined with any certainty. However, by comparing distributions given by a δ function, Maxwellian, and exponential forms, each with the same rms velocity, one obtains a variation in the mean speed of about 35%. As stated above, a value of k from the middle of this range was adopted.

C. Transition Strengths

The lifetimes of the $\frac{7}{2}^+$, $\frac{9}{2}^+$, and $\frac{11}{2}^+$ members of the multiplet are all less than 10^{-13} sec. The partial $E3$ lifetimes of the states for decay to the ground state can be estimated from the $B(E3)$ of the 3^- state in ^{208}Pb, assuming that the octupole-multiplet levels are indeed well described by weak-coupling wave functions. These $E3$ lifetimes are of the order of 2×10^{-11} sec. A single-particle $M2$ partial lifetime for decay of the levels to ground is of the order of 10^{-11} sec. Thus, little error is made in ascribing all of the transition probabilities of the $\frac{7}{2}^+$, $\frac{9}{2}^+$, and $\frac{11}{2}^+$ levels to the electric-dipole decay modes. The $B(E1)$ values for the decays of the three levels can then be calculated if one knows the fractions of the levels that decay via the transitions considered. In the cases of the $\frac{9}{2}^+$ and $\frac{11}{2}^+$ levels, upper limits only were placed on the lifetimes. These put lower limits on the $B(E1)$ values for the ground-state transitions from these levels, assuming the predominant decays of the states are to ground. In the case of the $\frac{7}{2}^+$ multiplet

TABLE III. Relative transition rates.

Transitions	Type	Method of measurement	Ratio Expt	Ratio Theory[a]
$0.897 \to GD/0.897 \to GD$	$E2/M1$	Ang. dist.	$0.7-1.3$	1.1
$1.608 \to 0.897/1.608 \to GD$	$E3/(E3+M2)$	γ-ray intensities	≤0.07	10^{-4}
$2.563 \to 0.897/2.563 \to GD$	$E1/(E1+M2+E3)$	γ-ray intensities	≤0.08	$0.08[k(\tau=1)=5.9]$
$2.563 \to 1.608/2.563 \to GD$	$E2/(E1+M2+E3)$	γ-ray intensities	≤0.20	$10^{-3}(k_\tau=5.5)$
$2.581 \to 0.897/2.581 \to GD$	$E1/(E1+M2+E3)$	γ-ray intensities	0.88 ± 0.08	$0.88(k_\tau=4.3)$
$2.598 \to 1.608/2.598 \to GD$[b]	$(M1+E2)/(E1+M2+E3)$	γ-ray intensities	1.25 ± 0.09	$1.25(k_\tau=6.3)$
$2.615 \to 0.897/2.615 \to GD$	$E1/(M2+E3)$	γ-ray intensities	$1.51_{-0.8}{}^{+0.4}$	$1.51(k_\tau=5.4)$
$2.615 \to GD/2.615 \to GD$	$E3/M2$	Ang. dist.	$0.8-25.0$	8
$2.740 \to 1.608/2.740 \to GD$	$(M1+E2)/E3$	γ-ray intensities	1.44 ± 0.18	3
$2.822 \to 0.897/2.822 \to GD$	$(M1+E2)/E2$	γ-ray intensities	<0.9	2

[a] For the $E1$ transitions, the strength parameter $k(\tau=1)$ was adjusted to give agreement with experiment (see text).
[b] Separate 11/2, 13/2$^+$ contributions unresolved.

[26] J. R. MacDonald, D. F. H. Start, R. Anderson, A. G. Robertson, and M. A. Grace, Nucl. Phys. **A108**, 6 (1968).

level, if it is assumed that the only decays of the level are to ground and to the 0.897-MeV state, then the measured lifetime gives the $B(E1)$ values shown in Table II for these transitions.

Other reduced matrix elements can be obtained from the observed Coulomb-excitation γ-ray yields. From Fig. 7, one can calculate the total number of upward excitations of the $f_{7/2}$, $i_{13/2}$, and $f_{5/2}$ levels during the bombardments. This cannot be done for the individual levels of the octupole multiplet, since there exist transitions between them which were not observed in this experiment. (These will mainly take place through internal conversion.) The total number of upward transitions to all the multiplet levels combined, however, can be obtained. These numbers may be compared with predictions to give the reduced matrix elements for the upward transitions. These are shown in Table II.
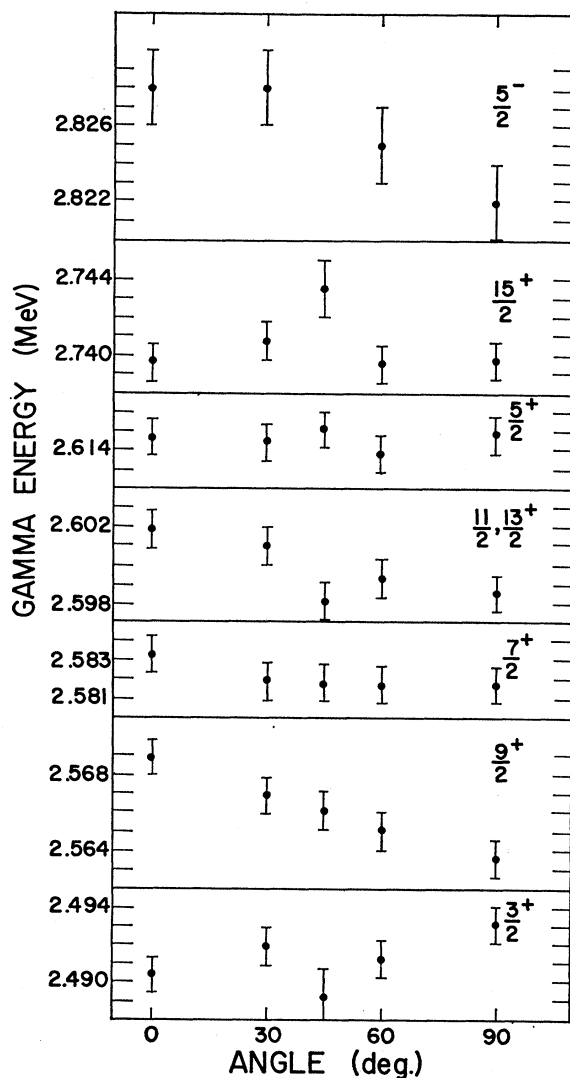
TABLE IV. Relative Coulomb-excitation yields.

Energy (MeV)	Assumed spin J	Calculated[a] yield	Observed yield
2.491	3/2	4.75	3.9 ± 0.4
2.563	9/2	10.47	$10.3_{-0.4}^{+2.7}$
2.581	7/2	8.1	9.3 ± 1.0
2.598	11/2, 13/2	25.5	24.8 ± 1.0
2.615	5/2	5.8	$8.3_{-2.7}^{+1.6}$
2.740	15/2	12.2	9.0 ± 0.7

[a] Assuming the total octupole strength of $0.57\ e^2b^3$ is distributed among the ^{209}Bi multiplet states according to the $(2J+1)$ rule. The units are those of Fig. 7.

It should be noted that the error introduced because of uncertainty in the detector efficiency is not included in Table II in order not to distort the accuracy to which the relative $B(E1)$ values determined from γ-intensity measurements are known. The $E3$ strength to all the multiplet levels combined is in excellent agreement with the $B(E3)$ of the 3$^-$ ^{208}Pb state.[18,27] The only other value that can sensibly be compared with previous experiments is the $B(E2)$ for the upward transition to the $f_{7/2}$ level at 0.897 MeV. This has been measured in poor-resolution experiments to be 1.3×10^{-3},[10] $(7 \pm 2) \times 10^{-3}$,[11] and $(3.2 \pm 0.7) \times 10^{-3}$ e^2b^2.[12]

The following points in the analysis of the γ-ray intensities need further comment:

(i) It is assumed that the $f_{5/2}$ level has no decay to any member of the multiplet. Dipole transitions could only proceed through admixtures in the states. These are expected to be small, whereas dipole strengths of at least 0.15 single-particle units would be required in order for branches to the multiplet to compete with the observed quadrupole decays of the $f_{5/2}$ level.

(ii) It is assumed that population of levels at excitation energies greater than 3 MeV in ^{209}Bi can be neglected. Of the levels above 3 MeV, the chief candidates for excitation are the set of levels formed by coupling the $h_{9/2}$ proton to the 2$^+$ core state of ^{208}Pb. If we assume that this set is a degenerate group at 4.0 MeV (the excitation of the 2$^+$ state in ^{208}Pb) that has the same quadrupole strength as the 2$^+$ level,[28] it is found that the number excited is less than 5% of the number of the octupole multiplet excited.

(iii) In calculating the thick-target yield for the levels of the octupole multiplet, it was assumed that only $E3$ excitation contributed. Magnetic excitation of the levels may be disregarded, but there is the possibility of $E1$ excitation of the $\frac{7}{2}^+$, $\frac{9}{2}^+$, and $\frac{11}{2}^+$ levels. The $B(E1)$ values for the downward transitions have been discussed above. Only in the case of the $\frac{7}{2}^+$ level

FIG. 10. Variation of observed γ-ray energy with detector angle for γ rays greater than 2.4 MeV from bismuth at 19 MeV.

[27] There exist several measurements of this quantity, but the value of 0.58 ± 0.04 is probably the best to use in Coulomb-excitation comparisons.

[28] J. F. Ziegler and G. A. Peterson, Phys. Rev. **165**, 1337 (1968).

TABLE V. Energy, reduced transition probability, and vibrational motion amplitude of the octupole, quadrupole, and dipole modes of the ^{208}Pb core. The parameter f_λ characterizes the strength of the particle-vibration coupling. In the estimate of f_λ, the radial integral $k(r)$ was set equal to 60 MeV [see Eq. (5)] for the quadrupole and octupole modes and equal to 300 MeV for the dipole case (see text).

λ^π	$\hbar w_\lambda$ (MeV)	$B(E\lambda; n_\lambda=0 \rightarrow n_\lambda=1)$ $\times e^2(10^{-24}\,\text{cm}^2)^\lambda$	$(hw_\lambda/2c_\lambda)^{1/2}$	f_λ
3^-	2.615	0.53[a]	4.2×10^{-2}	0.34
2^+	4.07	0.30[b]	2.5×10^{-2}	0.12
1^-	14	0.7[c]	3.9×10^{-2}	0.24

[a] Reference 18.
[b] Reference 28.
[c] See text.

is the $B(E1)$ value known with any certainty, but it is very unlikely that the $B(E1)$ for any of the upward transitions exceeds $10^{-4}\,e^2$b. Using such a value for $B(E1)$, it is found that the $E1$ contribution to the Coulomb excitation of a state at 2.6 MeV in ^{209}Bi that has a $B(E3)$ of 0.1 e^2b^3 is less than 1%.

In addition to the reduced matrix elements discussed above, there are several relative transition rates measured in the experiment that can be compared with the theoretically predicted values. These are shown in Table III. Most of them come in a straightforward manner from the relative γ-ray intensities shown on Fig. 7. Two of them arise from consideration of γ-ray angular distributions which are discussed in the Sec. III D.

D. Angular Distributions

The information that can be obtained from the angular distributions is limited because, apart from the $\frac{15}{2}^+$ and $\frac{5}{2}^+$ states, the decaying levels most probably have several paths by which they have been populated. Also, there is the possibility of mixing of different multipolarities in many of the downward γ transitions.

There is no angular distribution that cannot be sensibly fitted for the assumed spins of the multiplet levels. In Figs. 4–6, which show the angular distributions, the full lines drawn are for the four cases where the analysis may be expected to involve only a few parameters (discussed below). In each case, the full line was calculated using thin-target angular-distribution coefficients for the $E3$ excitation computed from formulas given in Alder *et al.*[17] The values for the thick-target coefficients were taken to be the thin-target ones evaluated at an energy smaller than the bombarding energy E_0 by the factor $(1+\delta E_3/E_0)$ with δE_3 taken from Ref. 17. A small correction was included to account for the finite solid angle subtended by the detector. The four angular distributions that involve only a few parameters are

(i) $\frac{15}{2}^+$ level to ground. It is assumed that the $\frac{15}{2}^+$

level is only populated by direct $E3$ Coulomb excitation and decays via a pure-$E3$ transition.

(ii) $\frac{5}{2}^+$ level to ground. It is again assumed that there is no feeding of the level from states above it. The γ ray is taken to be an $M2/E3$ mixture, and the line drawn is for an intensity ratio $(E3)^2/(M2)^2$ of 4/1, although the distribution in this case is relatively insensitive to the mixing ratio.

(iii) $\frac{5}{2}^+$ level to 0.897-MeV level. The curve drawn is for a pure electric-dipole transition downwards.

(iv) 0.897-MeV level to ground. In order to obtain a rough estimate of the $E2/M1$ mixing ratio in this transition, it is assumed that the angular distribution of the γ rays from the decay of those $f_{7/2}$ levels populated via branches from levels above is isotropic. This approximation is not too bad, since the angular distributions of most of the primary γ rays from the higher levels are not very anisotropic. We then subtract an isotropic part from the 0.897-MeV γ-ray data whose magnitude is known from the strengths of the branches from the higher levels:

The remaining angular distribution is analyzed as if the $f_{7/2}$ level were isolated and Coulomb excited by the quadrupole part of the electric field and deexcites via an $E2/M1$ mixture. The full curve drawn on Fig. 4 is the sum of the isotropic part and the second part, calculated for an intensity ratio $(E2)^2/(M1)^2$ of unity.

No information can be obtained from the angular distribution of the 1.608-MeV γ ray, since, in this case, most of the γ rays arise from levels that have been populated via decays from higher states.

E. Identification of Level Spins

The assignment of the 2.822-MeV peak as the $\frac{5}{2}^-$ single-particle level suggested by proton-transfer studies is not certain. The observed energy is near to previously measured values, but these latter have not been accurately determined. Nevertheless, there are several other factors that give plausibility to the assignment. The $f_{5/2}$ single-proton state is the only negative-parity state expected in this region that could be excited via $E2$ Coulomb excitation. Furthermore, enhancement of the $B(E2)$ is expected theoretically through mixing with the 2^+ core multiplet near 4 MeV, especially since the 0.897-MeV $f_{7/2}$ state is seen to be enhanced in this way. This point is discussed further in Sec. IV. The Doppler effects are quite consistent with a lifetime of less than 10^{-14} sec, which is an upper limit based on the measured $B(E2)$.

Evidence supporting the identification of the 3^- septuplet with the γ peaks seen near 2.6 MeV is overwhelming. It is based on the accurately known energies of the states and the excellent agreement with the expected total octupole strength. The spins were originally assigned somewhat tentatively, assuming the $(2J+1)$ rule for excitation via inelastic proton scattering at 21 MeV.[9] The following summarizes to what

extent the present work supports and verifies these assignments.

The calculated thick-target Coulomb-excitation yield for each level of the multiplet, based on the weak-coupling model, is given in column 3 of Table IV. In this calculation, the summed $B(E3)$ was taken to be the experimentally observed value of 0.57 e^2b^3. The observed yields are listed in column 4. In general the agreement is good.

The lowest multiplet member at 2.491 MeV is the weakest state, and its single branch to the ground state is consistent only with an assumed spin of $\frac{3}{2}$. The next most weak state is at 2.615 MeV, which is consistent with its $\frac{5}{2}$ spin assignment, although it could possibly be a stronger state that had lost some of its strength within the multiplet. This is unlikely, however, since its significant branch to the $\frac{7}{2}^-$ state at 0.897 MeV eliminates the higher spin values, and the $\frac{7}{2}^+$, $\frac{9}{2}^+$, and $\frac{11}{2}^+$ levels are marked as the Doppler-broadened lines at 2.581, 2.563, and 2.598 MeV. On the basis of the present results, it is not possible to determine unambiguously the spins of these latter states, although the branch to the 0.897-MeV state from the 2.581-MeV state indicates that the latter is almost certainty not $\frac{11}{2}^+$.

The uppermost member at 2.740 MeV decays to the 1.608-MeV state, suggesting a high spin. Indeed, the angular distribution of its ground-state branch is consistent with pure $E3$ excitation and decay assuming $J=\frac{15}{2}$ (see Fig. 6).

The discrepancy between the observed and calculated yields (Table IV), which is greatest for this state, is thought to be due mainly to the presence of an enhanced $M1$ transition to the $\frac{13}{2}^+$ multiplet state. Calculations indicate that this is the most important intermultiplet transition. The only other significant one, the $\frac{5}{2}^+$ to $\frac{7}{2}^+$ $M1$ transition, contributes less than the experimental uncertainty in the $\frac{5}{2}^+$ yield.

The absolute $M1$ transition rates are sensitive to the g factor of the octupole state.[29] However, the ratio of the $\frac{15}{2}^+$ to $\frac{13}{2}^+$ and $\frac{15}{2}^+$ to $i_{13/2}$ transition rates, both assumed to be $M1$, is sensitive only to the collective admixture in the 1.6-MeV state, which was taken to be 0.19 (see Table IX). Including the effect of internal conversion, the $\frac{15}{2}^+$ to $\frac{13}{2}^+$ rate is approximately 0.26 times that of the $\frac{15}{2}^+$ to $i_{13/2}$ transition, which reduces the discrepancy shown in Table IV to about 15% of the calculated yield.

Using the known magnetic moment of the ^{209}Bi ground state, the observed $\frac{15}{2}^+$ to $i_{13/2}$ $M1$ transition rate is given by a particle-vibration coupling calculation[30] if the g factor for the octupole state is taken to be 0.6, which agrees with a recent measurement of this quantity.[31]

[29] I. Hamamoto, Niels Bohr Institute, Copenhagen, report (unpublished).
[30] I. Hamamoto (private communication).
[31] J. D. Bowman, F. C. Zawislak, and E. N. Kaufmann, Phys. Letters **29B**, 226 (1969).

TABLE VI. Matrix elements of the radial form factor $k(r) = -r[dV(r)/dr]$. A Wood-Saxon single-particle potential was used with parameters $V_0 = -58.17$ MeV, $R_0 = 1.27A^{1/3}$ ($A = 209$), $a_0 = 0.67$ fm, $\chi_{1s} = 32$ MeV, which binds the $i_{13/2}$ state by -2.28 MeV. In this potential the $f_{5/2}$ level is unbound by 260 keV.

$n_2 l_2 j_2$	$n_1 l_1 j_1$	$-\langle n_2 l_2 j_2 \mid k(r) \mid n_1 l_1 j_1 \rangle$ (MeV)
$1f_{5/2}$	$1f_{5/2}$	58.9
	$0i_{13/2}$	64.5
	$1f_{7/2}$	59.5
	$0h_{9/2}$	48.2
$0i_{13/2}$	$0i_{13/2}$	77.4
	$1f_{7/2}$	63.4
	$0h_{9/2}$	61.4
$1f_{7/2}$	$1f_{7/2}$	60.7
	$0h_{9/2}$	46.3
$0h_{9/2}$	$0h_{9/2}$	50.8

In general, the over-all consistency between experiment and theoretical expectation, together with the evidence of the decay scheme of the multiplet, lends strong support to the original spin assignments of the states and the applicability of the weak-coupling theory.

As has already been pointed out, there is good evidence from other work that the peak at 2.598 MeV is due to a close doublet consisting of the $\frac{11}{2}^+$ and $\frac{13}{2}^+$ states. The present results strongly support this hypothesis. The observed strength is considerably larger than that expected for any single state. Furthermore, it would be most unusual for a single state to show a large and apparently undetectably broadened branch to the $i_{13/2}$ state at 1.608 MeV while at the same time decaying with a very short lifetime to ground.

A doublet separation of about 8 keV could account for the broadening, but not the observed Doppler shift. It is therefore concluded that one of the members, presumably the $\frac{11}{2}^+$, does indeed decay very quickly to ground. It is also plausible to assume that this state has no significant branches elsewhere. If this is so, the 2.598-MeV γ peak must be due mainly to the $\frac{11}{2}^+$ decay only, since the observed strength allows relatively little of the $\frac{13}{2}^+$ state to contribute. Also the branch to the 1.608-MeV state must be almost entirely due to the $\frac{13}{2}^+$ component.

Such a situation suggests a method for estimating the doublet separation by comparing the energy of the ground-state decay with the sum of the energies of the transitions $\frac{13}{2}^+$ to $i_{13/2}$ state and $i_{13/2}$ to ground. Using the energy values determined in this experiment, a value of 2.0 ± 1.5 keV is obtained for the doublet separation, with the $\frac{13}{2}^+$ state lying higher at 2.600 MeV.

IV. DISCUSSION

In what follows, we analyze the experimental results in terms of a proton moving in the single-particle orbits of the ^{208}Pb core and weakly coupled to its vibrational

TABLE VII. Some of the matrix elements used to construct the wave functions displayed in Table IX. The matrix elements that do not involve spin flip are typically four times larger than the ones involving spin flip (see text).

λ	j_2	j_1	$\langle (j_2\lambda)j_1 \mid H_2^{(c)} \mid j_1 \rangle$ (MeV)
3	$0i_{13/2}$	$0h_{9/2}$	-0.23
	$0i_{11/2}$	$0h_{9/2}$	0.79
	$0i_{13/2}$	$1f_{7/2}$	1.18
	$0i_{11/2}$	$1f_{7/2}$	0.29
2	$1f_{5/2}$	$0h_{9/2}$	-0.39
	$1f_{7/2}$	$0h_{9/2}$	0.08
	$0h_{9/2}$	$1f_{7/2}$	-0.11
	$0h_{9/2}$	$1f_{5/2}$	-0.50

modes. The very small splitting of the octupole multiplet makes it possible to describe these states in first approximation as simple vector-coupled products of the $h_{9/2}$ proton and the $\lambda^\pi = 3^-$ vibrational excitation. We shall see that it is necessary to include other collective and single particle degrees of freedom to account for the observed transition rates.

The coupling between the oscillating core and the extra particle[8] is

$$H_c^{(\lambda)} = k_\lambda(r) \sum_\mu Y_{\lambda\mu}^*(\theta, \phi) \alpha_{\lambda\mu}$$

$$= (-1)^\lambda k_\lambda(r) (2\lambda+1)^{1/2}(Y_\lambda \alpha_\lambda)_0, \quad (2)$$

where

$$\alpha_{\lambda\mu} = \int R(\theta, \phi) Y_{\lambda\mu}(\theta, \phi) \sin\theta \, d\theta d\phi$$

are the deformation parameters: $R(\theta, \phi)$ is the nuclear radius, and the spherical harmonics refer to the multipole moments of the particle motion. The radial form factor is given by

$$k_\lambda(r) = -r[dV(r)/dr]. \quad (3)$$

The basic matrix element associated with the coupling (2) describes a process involving the emission or absorption of a vibrational quantum

$$\langle (j_2\lambda)j_1 \mid H_c^{(\lambda)} \mid j_1 \rangle = i^{l_1+\lambda-l_2}(-1)^\lambda[(2\lambda+1)/4\pi]^{1/2}$$

$$\times \langle j_1\tfrac{1}{2}\lambda 0 \mid j_2\tfrac{1}{2}\rangle \langle j_2 \mid k_\lambda(r) \mid j_1 \rangle(\hbar\omega_\lambda/2c_\lambda)^{1/2}. \quad (4)$$

For example, the coupling $H_c^{(3)}$ mixes some of the state formed by coupling the $h_{9/2}$ proton to the 3^- mode into the predominantly $i_{13/2}$ state. The parameter $(\hbar\omega_\lambda/2c_\lambda)^{1/2}$ measures the amplitude of the vibrational motion. Employing the classical expression for the multipole moment of a uniformly charged drop, it is possible to relate the value of $(\hbar\omega_\lambda/2c_\lambda)^{1/2}$ to the reduced transition probability between ground state and the first vibrational state.[32] (See Table V.)

$$B(E\lambda; \eta_\lambda=0 \rightarrow \eta_\lambda=1) = [(3/4\pi)ZeR_0^\lambda]^2(2\lambda+1)$$

$$\times (\hbar\omega_\lambda/2c_\lambda). \quad (5)$$

[32] O. Nathan, in *Studies of Nuclear Quadrupole and Octupole Vibrations* (Munksgaard; Ejnar Mirnksgaard, Copenhagen, 1964).

In Table VI, we collect the values of $k = \langle j_2 \mid k_\lambda(r) \mid j_1 \rangle$ obtained using a Woods-Saxon single-particle potential to calculate $k_\lambda(r)$ and the R_{nlj}.

A simple consequence of the coupling (5) is that transitions involving spin flip are strongly reduced with respect to transitions that do not flip the spin (see Table VII). The influence of spin-dependent fields on the particle-core coupling has been studied in another work.[33]

The observed coupling in ^{209}Bi is weak. One can express this in a quantitative way by means of the dimensionless parameter

$$f_\lambda = [(2\lambda+1)/16\pi]^{1/2}(\hbar\omega_\lambda/2c_\lambda)^{1/2}(k/\hbar\omega_\lambda), \quad (6)$$

where f_λ measures the importance of mixing into the zero-order configurations; for example, it gives a rough estimate of the amount the $(h_{9/2}, 3^-)\frac{13}{2}^+$ configuration mixes into the predominantly $i_{13/2}$ single-particle state. For $f_\lambda \ll 1$, the coupling can be treated by a perturbation expansion. In Table V, the values of f_λ for $\lambda = 1, 2, 3$ are displayed, and it is seen that in ^{209}Bi we have a weak-coupling situation. In a perturbation expansion of the particle-vibration coupling, one obtains a first-order correction to transition moments between single-particle states. These renormalization effects of the single-particle moments are associated with both the dynamic and static moments of the vibrational mode. Because of the large values of the former, these renormalization effects are very important. The physical single-particle state can be written to first order in the coupling constant as

$$\mid nlj_1 \rangle' = \mid nlj_1 \rangle + \sum_{\lambda, j_2} \frac{\langle (j_2\lambda)j_1 \mid H_c^{(\lambda)} \mid j_1 \rangle}{\epsilon(j_1) - [\epsilon(j_2) + \hbar\omega_\lambda]} \mid (j_2\lambda)j_1 \rangle.$$

$$(7)$$

TABLE VIII. Single-particle energies used in the calculation of the first-order corrections to the single-particle wave functions.

nlj	E_{nlj} (MeV)
$0h_{9/2}$	0.0[a]
$1f_{7/2}$	0.897[a]
$0i_{13/2}$	1.608[a]
$1f_{5/2}$	2.822[a]
$2p_{3/2}$	3.1[a]
$2p_{1/2}$	3.6[a]
$1g_{9/2}$	3.9[b]
$0j_{15/2}$	5.9[b]
$0i_{11/2}$	6.2[b]
$1g_{7/2}$	7.5[b]
$2d_{5/2}$	8.2[b]

[a] Experimental energy.
[b] Spherical Nilsson model with parameters $\chi_p = 0.057$, $\mu_p = 0.65$.

[33] R. A. Broglia, J. Damgaard, and A. Molinari, Nucl. Phys. **A127**, 429 (1969).

TABLE IX. Wave functions of ^{209}Bi predicted by the weak-coupling model to first order in perturbation theory. The odd proton was allowed to move in the $0h_{9/2}$, $1f_{7/2}$, $0i_{13/2}$, $1f_{5/2}$, $2p_{3/2}$, $2p_{1/2}$, $1g_{9/2}$, $0j_{15/2}$, $0i_{11/2}$, $1g_{7/2}$, and $2d_{5/2}$ single-particle orbits, and the ^{208}Pb core to be either in the ground state or in an excited-dipole, -quadrupole, or -octupole mode of vibration.

nlj, λ	$9/2^-$ (0.000)	$7/2^-$ (0.897)	$13/2^+$ (1.608)	$3/2^+$ (2.491)	$9/2^+$ (2.563)	$7/2^+$ (2.581)	$11/2^+$ (2.598)	$13/2^+$ (2.600)	$5/2^+$ (2.615)	$15/2^+$ (2.740)	$5/2^-$ (2.822)
$0h_{9/2}$	1.000										
$1f_{7/2}$		1.000									
$0i_{13/2}$			1.000					0.1921			
$1f_{5/2}$											1.000
$1g_{9/2}$					-0.2110						
$0i_{11/2}$							-0.1973				
$1g_{7/2}$						-0.1582					
$2d_{5/2}$									-0.0529		
$0h_{9/2}3$			-0.1921	1.000	1.000	1.000	1.000	1.000	1.000	1.000	
$1f_{7/2}3$			-0.4692		-0.3759	0.0137	0.0166	-0.0901	-0.0068		
$0i_{13/2}3$	0.0542	-0.3553									
$1f_{5/2}3$					0.0387	-0.0508	-0.2115		-0.0063		
$2p_{3/2}3$					0.089	0.034			-0.005		
$2p_{1/2}3$						-0.081			-0.006		
$1g_{9/2}3$	0.0416	-0.1376									0.0987
$0j_{15/2}3$			-0.1121		0.0501		-0.0160	-0.0215			
$0i_{11/2}3$	-0.0879	-0.0349									-0.1923
$1g_{7/2}3$	-0.0683	-0.0375									-0.1048
$2d_{5/2}3$	0.0233	-0.0590									0.0620
$0h_{9/2}2$	0.0969	0.0338									0.4213
$1f_{7/2}2$	-0.0193	0.1148									-0.0855
$0i_{13/2}2$			0.1488		-0.0745		-0.0354	0.0286			
$1f_{5/2}2$	0.0589	0.0264									0.1091
$2p_{3/2}2$		0.077									-0.052
$2p_{1/2}2$											0.087
$1g_{9/2}2$			0.0834		-0.0241	0.0469	0.0114	0.0160	0.0226		
$0i_{11/2}2$			0.0100		-0.0037	-0.0364	-0.0227	0.0019			
$1g_{7/2}2$					-0.0034	-0.0180	-0.0191		-0.0047		
$2d_{5/2}2$					-0.0131	0.0042			-0.0059		
$0h_{9/2}1$					-0.0065	-0.0558	-0.0525				
$1f_{7/2}1$					-0.0394	-0.0083			-0.0253		
$1f_{5/2}1$						-0.0342			-0.0042		
$2p_{3/2}1$									-0.009		
$1g_{9/2}1$	-0.0173	0.1498									
$0i_{15/2}1$								0.0262			
$0i_{11/2}1$	0.1125										
$1g_{7/2}1$	0.0954	0.0209									0.1384
$2d_{5/2}1$		0.0990									-0.0301

TABLE X. The most important contributions to the $B(E\lambda)$ values associated with the transitions listed in the first column.

$0 \to 1.608$

$$\begin{cases} \langle 0i_{13/2} \| i^3\mathfrak{M}(E3) \| 0h_{9/2} \rangle = 0.072 \times 10^{-36}\ e\ \mathrm{cm}^3 \\ \langle (0h_{9/2}3^-)13/2 \| i^3\mathfrak{M}(E3) \| 0h_{9/2} \rangle = -1.10 \times 10^{-36}\ e\ \mathrm{cm}^3 \\ \langle 0i_{13/2} \| i^3\mathfrak{M}(E3) \| (0i_{13/2}3^-)\tfrac{9}{2} \rangle = 0.87 \times 10^{-36}\ e\ \mathrm{cm}^3 \end{cases}$$

$0 \to 0.897$

$$\begin{cases} \langle 1f_{7/2} \| i^2\mathfrak{M}(E2) \| 0h_{9/2} \rangle = 0.04 \times 10^{-24}\ e\ \mathrm{cm}^2 \\ \langle (0h_{9/2}2^+)\tfrac{7}{2} \| i^2\mathfrak{M}(E2) \| 0h_{9/2} \rangle = 0.69 \times 10^{-24}\ e\ \mathrm{cm}^2 \\ \langle 1f_{7/2} \| i^2\mathfrak{M}(E2) \| (f_{7/2}2^+)\tfrac{9}{2} \rangle = -0.77 \times 10^{-24}\ e\ \mathrm{cm}^2 \end{cases}$$

$0 \to 2.822$

$$\begin{cases} \langle 1f_{5/2} \| i^2\mathfrak{M}(E2) \| 0h_{9/2} \rangle = 0.18 \times 10^{-24}\ e\ \mathrm{cm}^2 \\ \langle (0h_{9/2}2^+)\tfrac{5}{2} \| i^2\mathfrak{M}(E2) \| 0h_{9/2} \rangle = 0.3 \times 10^{-24}\ e\ \mathrm{cm}^2 \\ \langle (1f_{5/2} \| i^2\mathfrak{M}(E2) \| (1f_{5/2}2^+)\tfrac{9}{2} \rangle = 0.8 \times 10^{-24}\ e\ \mathrm{cm}^2 \end{cases}$$
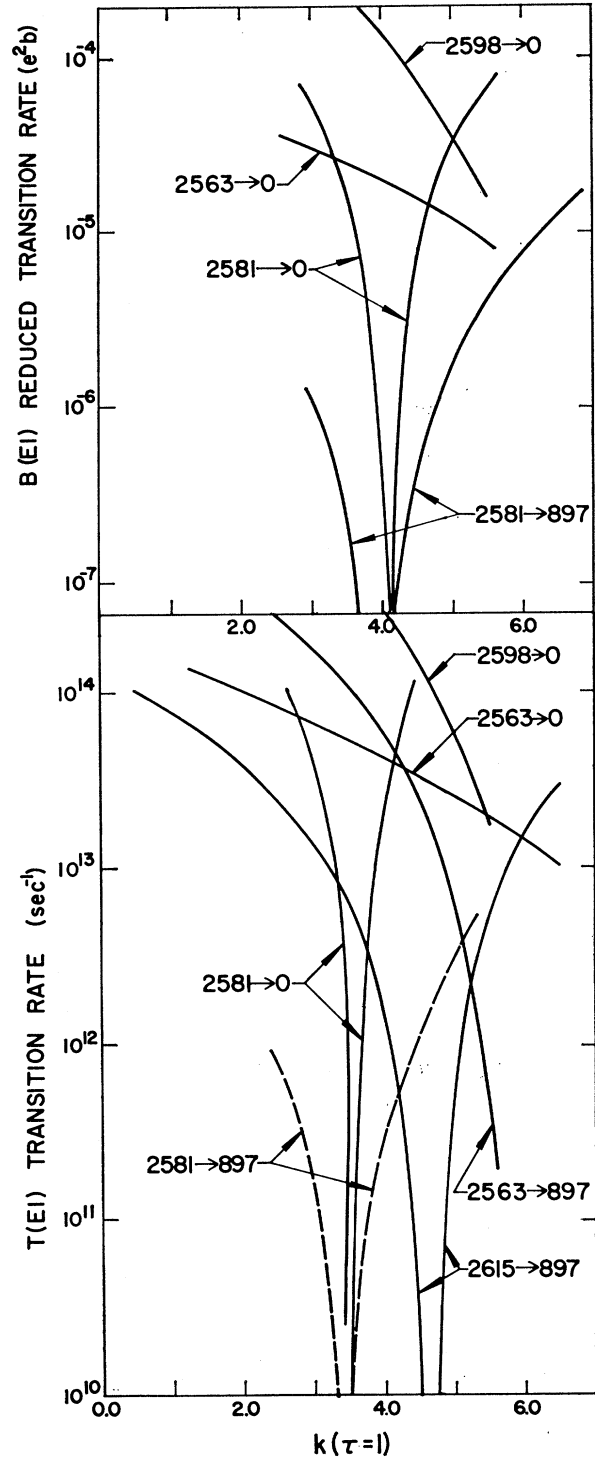
FIG. 11. Theoretical estimates of the reduced transition probabilities $B(E1)$ and the transition rates $T(E1)$ for the indicated transitions as a function of the coupling strength $k(\tau=1)$.

In what follows, we concentrate our attention on the predictions concerning transition probabilities. The energy shifts implied by the model have been discussed in Refs. 8 and 33. The multipole operator is expressed as

$$\mathfrak{M}(E\lambda, \mu) = (3Ze/4\pi)R_0^\lambda \alpha_{\lambda\mu}$$
$$+ \sum_k e[1-t_z(k)]r_k^\lambda Y_{\lambda\mu}(\theta_k\phi_k). \quad (8)$$

The corresponding reduced matrix element is

$$\langle (j_1\lambda)j \,||\, i^k\mathfrak{M}(Ek) \,||\, (j_1'\lambda')j'\rangle$$

$$= (-1)^{j+j_1+\lambda+k} \begin{Bmatrix} j_1 & j_1' & k \\ j' & j & \lambda \end{Bmatrix} (2j+1)^{1/2}(2j'+1)^{1/2}$$

$$\times \langle j_1 \,||\, i^k\mathfrak{M}(Ek) \,||\, j_1'\rangle\delta(\lambda, \lambda')$$

$$+ (-1)^{j_1+\lambda'+j+k} \begin{Bmatrix} \lambda & \lambda' & k \\ j' & j & j_1 \end{Bmatrix}$$

$$\times (2j+1)^{1/2}(2j'+1)^{1/2}\langle \lambda \,||\, i^k\mathfrak{M}(Ek) \,||\, \lambda'\rangle\delta(j_1, j_1').$$
$$(9)$$

The reduced matrix element $\langle \lambda \,||\, i^k\mathfrak{M}(Ek) \,||\, \lambda'\rangle$ between a state with zero phonons and a state with one phonon is related to the corresponding reduced transition probability through

$$\langle \lambda \,||\, i^\lambda\mathfrak{M}(E\lambda) \,||\, 0\rangle = \langle 0 \,||\, i^\lambda\mathfrak{M}(E\lambda) \,||\, \lambda\rangle$$
$$= (-)^\lambda[B(E\lambda; 0{\to}\lambda)]^{1/2}. \quad (10)$$

We start by coupling the $h_{9/2}$ proton to the octupole mode and disregard any other degree of freedom (approximation I). The single-particle energies are listed in Table VIII. The corresponding wave functions can be obtained by selecting only the appropriate portions from Table IX. In Table II, we compare the predicted transition probabilities with the experimental ones. The $E3$ transition to the 1.608-MeV state has contributions from the single-particle component of the states and from the octupole admixtures. The corresponding reduced matrix elements are displayed in Table X. As expected for a degree of freedom associated with an attractive field, all the contributions have the same sign[8] (see the corresponding amplitudes involved in these transitions in Table IX). The agreement with experiment is very good.

With the same approximation I for the wave functions, Table II shows that the predicted $B(E2)$ values are a factor of 8 smaller than the experimental ones, and that the $B(E1)$ values for the $\frac{7}{2}^+$ to ground, and $\frac{7}{2}^+$ to $f_{7/2}$ transitions are too large by factors of about 1000 and 100, respectively. Thus, although the main energy pattern of the states below 2.83 MeV can be accounted for by coupling the $h_{9/2}$ proton to the octupole vibration of the core, the picture is clearly incomplete. We need to include the specific degrees of freedom

associated with the quadrupole and dipole core vibrations.

The first $J^\pi = 2^+$ state in ^{208}Pb appears at 4.07 MeV. It is excited in inelastic electron scattering with a reduced transition probability of eight single-particle units.[28] The associated amplitude of the vibrational motion is given in Table V. The photoabsorption in ^{208}Pb is concentrated in a relatively narrow energy range around $E_{\text{res}} = 14$ MeV and its width at half-maximum is $\Gamma \approx 4$ MeV.[34] The total oscillator strength associated with the photoabsorption may be obtained from the integrated cross section. If one treats the absorption as due to a single resonance, one obtains $\Gamma_\lambda = 64$ keV and a $B(E1)$ for the 1^- to ground state transition of $0.23 e^2 b$.

The matrix element associated with the coupling of a particle to an isospin-dependent oscillation with spin, isospin, and multipole quantum numbers $\sigma = 0$, $\tau = 1$, $\lambda = 1$ is

$$\langle (j_2 1^-) j_1 \mid H_c^{(1)} \mid j_1 \rangle = -i^{l_1 - l_2 + 1} k (\tau = 1)$$

$$\times \langle j_1 \tfrac{1}{2} \, 1 \, 0 \mid j_2 \tfrac{1}{2} \rangle. \quad (11)$$

The coupling strength $k(\tau = 1)$ can be related to the isospin-dependent part of the nuclear potential. In the present calculation, we have taken it as a parameter.

We considered the interaction to be repulsive. To obtain the wave functions displayed in Table IX, the odd proton was allowed to move in the $0h_{9/2}$, $1f_{7/2}$, $0i_{13/2}$, $1f_{5/2}$, $2p_{3/2}$, $2p_{1/2}$, $1g_{9/2}$, $0j_{15/2}$, $0i_{11/2}$, $1g_{7/2}$, and $2d_{5/2}$ single-particle orbits and the core to be in either the ground state or in an excited-dipole, -quadrupole, or -octupole mode of vibration. The corresponding reduced transition probabilities in comparison with experiment are displayed in Table II, column 6. In all the transitions considered, the reduced matrix element is built out of two contributions, the single-particle one and the one involving the creation or annihilation of a vibrational quantum. In the $E1$ case, these two contributions always have opposite signs. This result was to be expected from the fact that the giant-dipole resonance lies at a higher energy than the unperturbed shell-model estimate and that the transition strength is concentrated in this high-lying state at the expense of the low-lying noncollective states.

The fact that the total reduced matrix element associated with an $E1$ transition is equal to a small number (typically of the order of 10^{-2} efm) which is the difference between two large numbers of order of 1 efm, makes the $B(E1)$ values depend very strongly upon $k(\tau = 1)$. In Fig. 11, we display the theoretical estimates of both $B(E1)$ and the transition rates $T(E1)$ corresponding to the measured transitions, as a function of $k(\tau = 1)$. It is seen (see also Tables II and III) that

[34] J. S. Levinger, in *Nuclear Photo-disintegration* (Oxford University Press, New York, 1960); M. Danos and E. G. Fuller, Ann. Rev. Nucl. Sci. **15**, 29 (1965).

TABLE XI. Some of the reduced single-particle matrix elements that can be renormalized by the existence of a static quadrupole moment in the octupole vibration of ^{208}Pb. $M1$ and $M2$ represent the single-particle and collective contributions, respectively, in units of $10^{-24}\,e$ cm^2.

j	I	I'	$\langle (j3^-)I \mid\mid i^2 M(E2) \mid\mid (j3^-)I' \rangle$ $M1$	$M2$	Total
$0i_{11/2}$	$\tfrac{5}{2}$	$\tfrac{9}{2}$	0.07	0.74	0.81
$1f_{7/2}$	$\tfrac{5}{2}$	$\tfrac{9}{2}$	0.06	0.99	1.05
$0i_{13/2}$	$\tfrac{7}{2}$	$\tfrac{9}{2}$	-0.19	-0.19	-0.37
$0i_{11/2}$	$\tfrac{7}{2}$	$\tfrac{9}{2}$	-0.23	-0.38	-0.61

there is not a single value of $k(\tau = 1)$ that can reproduce all the experimental results except a region of agreement around $k(\tau = 1) = 5.2 \pm 1.0$.

A recent calculation[29] of the decay scheme of the septuplet in ^{209}Bi gives a more complete treatment of the $E1$ transitions than that described above. The influence of the giant-dipole resonance is taken into account through an effective charge $e_{\text{eff}}(E1) = 0.3$. The corresponding values of the $B(E1)$ reduced transition probabilities are in good agreement with the experimental results.

The $B(E2)$ reduced matrix elements associated with the ground state (g.s.)$\rightarrow$0.897 MeV, and with the g.s.$\rightarrow$2.822 MeV transitions are built up mainly by three coherent contributions, as was found before for the octupole excitation of the $\mid 0i_{13/2} \rangle'$ state. (See Table X.) In working out the $B(E2)$ matrix elements, we have taken into account the fact that the $J^\pi = 3^-$ state of ^{208}Pb has a static quadrupole moment[19] $Q \approx -1 \times 10^{-24}$ cm^2. By means of the relation

$$\left(\frac{5}{16\pi} \right)^{1/2} Qe = \langle I \mid\mid \mathfrak{M}(E2) \mid\mid I \rangle$$

$$\times \left(\frac{I(2I-1)}{(2I+1)(I+1)(2I+3)} \right)^{1/2}, \quad (12)$$

we obtain

$$\langle 3^- \mid\mid \mathfrak{M}(E2) \mid\mid 3^- \rangle = -1.3 \times 10^{-24} e \text{ cm}^2. \quad (13)$$

The existence of a static quadrupole moment has the effect of renormalizing the single-particle transitions of the type

$$M = \langle (j, 3^-)I \mid\mid i^2 \mathfrak{M}(E2) \mid\mid (j, 3^-)I' \rangle.$$

In Table XI, we display the value of some of these matrix elements, showing the contribution arising from the static quadrupole moment of the 3^- vibration. The total matrix element is given by

$$\langle (j3^-)I \mid\mid i^2 \mathfrak{M}(E2) \mid\mid (j3^-)I' \rangle = M_1 + M_2,$$

where

$$M_1 = -(-1)^{I+j} \begin{Bmatrix} j & j & 2 \\ I' & I & 3 \end{Bmatrix} [(2I+1)(2I'+1)]^{1/2}$$

$$\times \langle j \mid\mid i^2 \mathfrak{M}(E2) \mid\mid j \rangle$$

is the single-particle contribution, and

$$M_2 = -(-1)^{j+I} \begin{Bmatrix} 3 & 3 & 2 \\ I' & I & j \end{Bmatrix} [(2I+1)(2I'+1)]^{1/2}$$
$$\times \langle 3^- || \mathfrak{M}(E2) || 3^- \rangle$$

represents the collective contribution. These matrix elements may be compared with the largest matrix element contributing to the different transitions. Compare, for example, the value of

$$\langle (0i_{11/2}3^-)\tfrac{5}{2} || i^2\mathfrak{M}(E2) || (0i_{11/2}3^-)\tfrac{9}{2} \rangle$$

(Table XI) with the value of

$$\langle 1f_{5/2} || i^2\mathfrak{M}(E2) || 0h_{9/2} \rangle,$$

$$\langle (0h_{9/2}2^+)\tfrac{5}{2} || i^2\mathfrak{M}(E2) || 0h_{9/2} \rangle,$$

and

$$\langle 1f_{5/2} || i^2\mathfrak{M}(E2) || (1f_{5/2}2^+)_{9/2} \rangle$$

(Table X). On the other hand, the contribution of

$$\langle (0i_{11/2}3^-)\tfrac{5}{2} || i^2\mathfrak{M}(E2) || (0i_{11/2}3^-)\tfrac{9}{2} \rangle$$

to the total matrix element is reduced by the product of the amplitudes with which the states $|(0i_{11/2}3^-)\tfrac{9}{2}\rangle$ and $|(0i_{11/2}3^-)\tfrac{5}{2}\rangle$ are mixed into the $|0h_{9/2}\rangle'$ and $|1f_{5/2}\rangle'$ levels, respectively. This number is of order 10^{-2}. As this is the case for all contributions of type M, the fact that $\langle 3^- || \mathfrak{M}(E2) || 3^- \rangle \neq 0$ affects the total transition probability by less than 3%. The same is true if one assumes that the quadrupole mode also has a static quadrupole moment of order of a single particle.

V. CONCLUSIONS

We can conclude that the particle-vibrator coupling scheme implied by the Hamiltonian (2) is extremely successful in describing the electromagnetic properties of the low-lying spectrum of ^{209}Bi. There is strong evidence that this is also true for all the other odd nuclei built taking ^{208}Pb as core.

In the case of $E1$ transitions, only a crude estimate of the effects of coupling the odd proton to the giant-dipole resonance has been presented. The present investigation shows that this degree of freedom must be introduced to get agreement with experiment. In a more refined calculation, the states in the continuum should be treated properly, and the $k(\tau=1)$ coupling constant derived from the isospin-dependent part of the nuclear potential.

The model also predicts spectroscopic factors for one-particle transfer reactions, e.g., ^{208}Pb$(^3$He, $d)^{209}$Bi. These numbers can be obtained from Table IX assuming ^{208}Pb(0) to be an inert core. However, because of the influence of the continuum states, in the one-particle form factors entering in the DWBA integrals, these numbers can only be considered as a qualitative estimate.